Real-time monitoring of a dynamic molecular system using ^{1}H-^{13}C HSQC NMR spectroscopy with an optimized ^{13}C window†

Giulio Gasparini,‡[a] Bruno Vitorge,‡[b] Paolo Scrimin,[a] Damien Jeannerat*[b] and Leonard J. Prins*[a]

Received (in Cambridge, UK) 21st February 2008, Accepted 17th March 2008
First published as an Advance Article on the web 21st April 2008
DOI: 10.1039/b803074j

The kinetic and thermodynamic parameters of an equilibrating network involving 8 molecules can be determined from a series of quick and highly resolved ^{1}H-^{13}C HSQC NMR experiments obtained using a reduced carbon spectral window.

Complexity is an emerging concept in chemistry, evidenced by a shift from the study and manipulation of individual molecules towards complex networks of interacting molecules.[1] Very recently, Ludlow and Otto made an enthusiastic plea for chemists to enter into this emerging field, called systems chemistry.[2] Examples ranging from dynamic combinatorial chemistry,[3] self-replication,[4] oscillating chemical reactions,[5] to models of biological networks[6] were used to illustrate the new properties and challenges that emerge from such systems. Consequently, analytical methods that permit a rapid and continuous monitoring of both the network composition *and* the reaction pathways are of eminent importance. For this purpose NMR spectroscopy is probably the most informative tool, since it is one of the few techniques that potentially allows a direct identification and quantification of all species present in solution as a function of time.[7] However, the application of NMR spectroscopy for studying mixtures of molecules is often severely hampered by overlapping signals and difficulties in signal assignment. Here, we show that these problems can be completely solved by monitoring the dynamic system with a series of quick and highly resolved ^{1}H-^{13}C HSQC NMR experiments. The experimental procedure relies on the reduction of the spectral width in the ^{13}C dimension of HSQC in order to enhance the resolution of signals *and* on a gradual increase in complexity of the system. From a single mixing experiment, the complete kinetic and thermodynamic picture of an eight-component network involving twelve exchange reactions can be obtained. In addition, this procedure allows for a direct monitoring of the adaptive behavior of the system towards an environmental change.

The dynamic network used to validate the application of ^{1}H-^{13}C HSQC NMR spectroscopy consists of four hydrazones **1A–1D**, which are in exchange due to the presence of the four hydrazides **A–D** (Scheme 1). Our interest in this kind of system arises from the observation that the thermodynamic equilibrium in this network is affected by the occurrence of intramolecular interactions between the phosphonate group and the functionality present in the hydrazide unit.[8] Since the phosphonate group is a transition state analog of the basic hydrolysis of an ester, identification of stabilizing interactions reveals which functional group can assist in catalysis. Recently, we have indeed shown that a correlation exists between the thermodynamic amplification and the efficiency in assisting in intramolecular catalysis.[9]

Previously, we have shown that the thermodynamic composition of a dynamic library containing nine different hydrazones

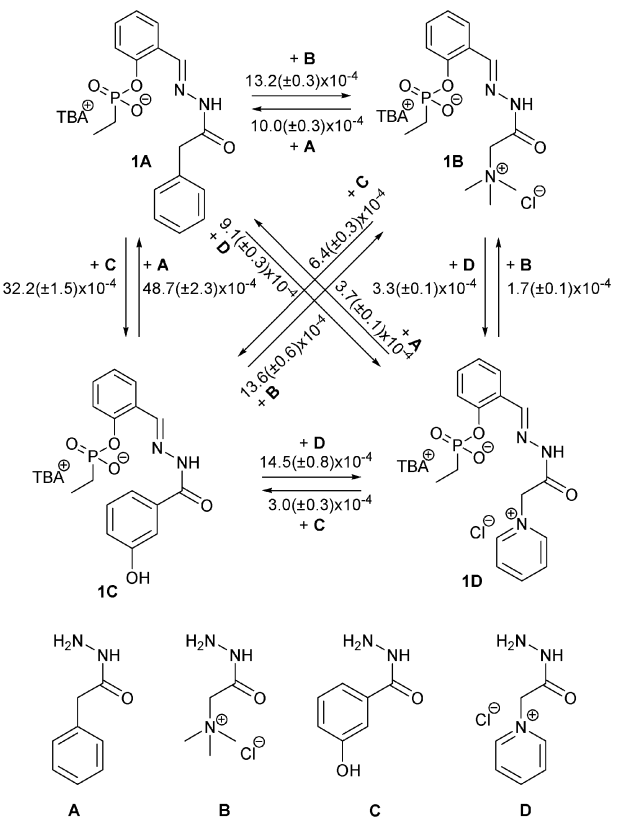

Scheme 1 Dynamic eight-component network containing four hydrazones **1A–1D** and four hydrazides **A–D** accounting for a total of twelve exchange reactions. Rate constants are calculated by fitting the kinetic profiles of Fig. 2. Each sections 1–3 is fitted separately, fixing the rate constants obtained from the previous section. That is, section 1 yields two rate constants $k_{\mathbf{1A}\rightarrow\mathbf{1B}}$ and $k_{\mathbf{1B}\rightarrow\mathbf{1A}}$ which are fixed for the fitting of section 2, which adds four new rate constants. Likewise, in section 3 six new rate constants are obtained.

[a] *Department of Chemical Sciences and CNR ITM Padova Section, University of Padova, via Marzolo 1, I-35131 Padova, Italy. E-mail: leonard.prins@unipd.it; Fax: +39 049 8275239; Tel: +39 049 8275256*
[b] *Department of Organic Chemistry, University of Geneva, 30 Quai E Anserment, Geneva, CH-1211, Switzerland. E-mail: Damien.Jeannerat@chiorg.unige.ch*

† Electronic supplementary information (ESI) available: Characterization data for hydrazones **1C** and **1D**, procedure for measuring the ^{1}H-^{13}C HSQC NMR spectra, quantification of signals in the HSQC spectra and Scientist model files for fitting the kinetics. See DOI: 10.1039/b803074j

‡ Authors G.G. and B.V. contributed equally to this work.

can be quantitatively determined using ^{1}H-^{13}C HSQC NMR spectroscopy.[9] The use of the ^{13}C dimension turned out to be essential in order to unequivocally identify all hydrazones present, since spectral overlap occurred in the 1D ^{1}H NMR spectrum. Nonetheless, signal assignment in the 2D NMR spectrum was impossible without having the ^{1}H and ^{13}C spectra of the pure hydrazones at hand. Here we show that this problem can be solved by following the kinetics of exchange directly by ^{1}H-^{13}C HSQC NMR measurements. ^{1}H-^{13}C HSQC NMR kinetic measurements become possible by using a spectral width in the ^{13}C dimension optimized for the carbon 'fingerprint' area of the individual hydrazones. This reduces the number of time increments needed to resolve the signals by one or two orders of magnitude and, as a consequence, also the experimental time.[10]

Hydrazides **A** and **B** were chosen because their behavior was well-known from a detailed previous study.[8] Hydrazide **C** exchanges at a much higher rate and thus enlarges the kinetic interval explored. Finally, hydrazide **D** forms a true challenge since additional signals are present in the 'fingerprint' area originating from the *o*- and *p*-protons of the pyridinium ring. The key trick in the experimental procedure is the sequential increase in complexity. So, the starting point is a 58 mM solution of hydrazone **1A** in CD_3OD which has two signals in the 'fingerprint' area (^{1}H: 7.8–9.2 ppm, ^{13}C: 142.6–147.4 ppm) corresponding to the *anti* and *syn* isomers with respect to the amide bond (**1A$_M$** and **1A$_m$**, Fig. 1a).[11] Addition of one equiv. of **A** and two equiv. of **B** results in the instalment of an equilibrium between **1A** and **1B**, evidenced by the appearance of two new signals in the 'fingerprint' area (**1B$_M$** and **1B$_m$**, Fig. 1b) and a concomitant decrease in intensity of signals **1A$_M$** and **1A$_m$**.§ Monitoring of the signal intensities as a function of time yields the rate profile for equilibration (section 1, Fig. 2), from which two second-order rate constants ($k_{\mathbf{1A\rightarrow 1B}}$ and $k_{\mathbf{1B\rightarrow 1A}}$) can be determined. The importance of using the ^{13}C dimension is illustrated by the separation of signals **1B$_M$** and **1A$_m$** in this dimension, whilst these overlap in the ^{1}H dimension.

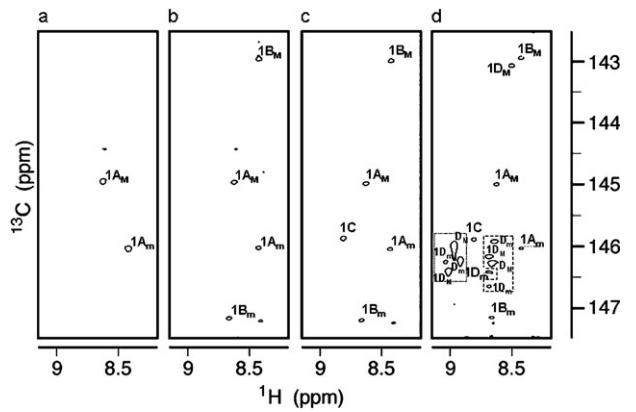

Fig. 1 ^{1}H-^{13}C HSQC NMR spectra (600 MHz, CD_3OD, 303 K) of the 'fingerprint' area at different times (t = 0 (a), 4 (b), 8 (c), and 13 (d) h, Fig. 2). The *o*- and *p*-protons of **1D** and **D** reside in the encircled areas in Fig. 1D. Each spectrum was obtained in 8 min using 400 time increments, 4.951 ppm (747.2 Hz) carbon spectral width and one scan per increment. The processing involved sine square processing after zero filling to 1024 points.¶

After four hours, two equivalents of hydrazide **C** are added resulting in the formation of hydrazone **1C** on the account of both **1A** and **1B**. The kinetic profile of **1A** is very interesting as it initially decreases rapidly and subsequently increases again to reach a constant value at thermodynamic equilibrium (inset of Fig. 2). Analysis of the rate constants shows that **C** reacts 5.0× faster with **1A** compared to **1B** ($k_{\mathbf{1A\rightarrow 1C}} = 32.2 \times 10^{-4}$ *vs* $k_{\mathbf{1B\rightarrow 1C}} = 6.4 \times 10^{-4}$ M^{-1} s^{-1}), which corresponds to a difference in activation energy $\Delta\Delta G^{\ddagger}$ of 3.8 kJ mol^{-1}. However, compared to hydrazone **1C**, **1B** is thermodynamically more stable than **1A** by 0.7 kJ mol^{-1} ($\Delta\Delta G_{\mathbf{1C-1A}} = 1.0$ *vs.* $\Delta\Delta G_{\mathbf{1C-1B}} = 1.7$ kJ mol^{-1})‖, which explains the subsequent increase in concentration of **1A**.

Finally, two equivalents of hydrazide **D** are added which installs the complete network as given in Scheme 1. Hydrazide **D** poses a challenge as the *o*- and *p*-protons of the pyridinium-ring resonate within the 'fingerprint' area, which is additionally complicated due to the presence of two isomeric forms of **D**. Given the fact that hydrazone **1D** is also present in two isomeric forms, a total of ten new signals appear (which include the two imine protons of both isomers of **1D**). Consequently, signal identification from a single ^{1}H-^{13}C HSQC spectrum as shown in Fig. 1d is essentially impossible. However, having the kinetic profile of each separate signal at hand, signal identification becomes very straightforward. First, signals are divided in two groups depending whether they increase or decrease in intensity. Four out of ten signals decrease in intensity, which by necessity means that these must result from hydrazide **D**, which is being consumed. These four signals can be further divided in two sets of two signals in a 2 : 1 ratio corresponding to the *o*- and *p*-protons of the major (**D$_M$**) and minor (**D$_m$**) isomers of hydrazide **D**. Based on their intensities, the six positive signals can also be grouped in two sets of three signals, which correspond to the major (**1D$_M$**) and minor (**1D$_m$**) isomers of hydrazone **1D**. The relative ratio of 2 : 1 : 1 for the three signals within each set is consistent with the ratio between *o*-, *p*-, and imine protons. The imine-signal of **1D$_M$** can be unambiguously assigned based on the ^{13}C

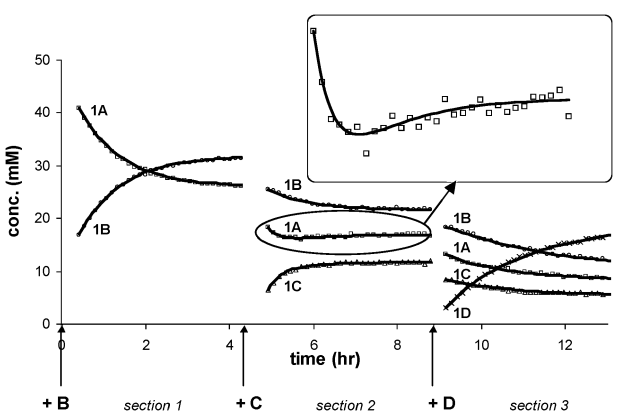

Fig. 2 Concentrations of hydrazones **1A** (□), **1B** (○), **1C** (Δ) and **1D** (×) as measured by ^{1}H-^{13}C HSQC NMR spectroscopy (600 MHz, CD_3OD, 303 K) throughout the mixing experiment. At the beginning of each section, two equivalents of **B**, **C**, and **D** (with respect to the scaffold **1**) are added, respectively, and the evolution of the system is followed kinetically. The solid lines represent the best fits to the appropriate models (see ESI†).

chemical shift of 143.074 ppm which falls out of the aromatic region. The imine-signal of $\mathbf{1D_m}$ cannot be discriminated from the *p*-proton, but for the system analysis this is of less importance as both have identical intensities.**,†† The peak assignment was fully confirmed by conventional 2D NMR measurements based on DQF-COSY, NOESY and HMBC.

The sequential increase in complexity allows for an accurate determination of all rate constants by fitting each section separately fixing the rate constants obtained from the previous sections. This way twelve rate constants were obtained with a maximum error of 9.4% for $k_{\mathbf{1D\rightarrow 1C}}$ ($(3.0 \pm 0.3) \times 10^{-4}\ M^{-1}\ s^{-1}$) (Scheme 1). An additional advantage of measuring the kinetics of the system is the possibility to calculate the composition of the system at thermodynamic equilibrium *via* extrapolation of the kinetic profile. This significantly reduces the experimental time, especially in situations where the thermodynamic equilibrium is reached very slowly. So, the kinetic profile of section 3 in Fig. 2 was extrapolated to give the equilibrium concentrations of hydrazones **1A–1D** ([**1A**] : [**1B**] : [**1C**] : [**1D**] = 19 : 25 : 13 : 43) from which the $\Delta\Delta G$ values were calculated as given in Fig. 3 with a maximum error of 14% (for $\Delta\Delta G_{\mathbf{1A-1B}}$).

Previous studies have shown that the thermodynamic stabilities of these hydrazones may depend on their concentration.[8] We were interested to find out whether this analytical tool allows us to detect changes in the mixture composition upon dilution. Therefore, the final mixture ([**1**] = 43 mM) was diluted to a final concentration of 5 mM and changes in the signal intensities were monitored for 24 h (see ESI†). In complete accordance with our previous results,[8,9] we observed an amplification of hydrazones **1B** and **1D** on the expense of hydrazones **1A** and **1C** upon dilution. Also the extent of amplification (**1B** > **1D**) is in line with our expectations. Obviously, dilution has brought us to the lower limits accessible with 2D NMR spectroscopy, which is around 0.5 mM for this spectrometer and probehead (600 MHz, TXI-cryoprobe), illustrated by the relative large errors.

The results presented here clearly illustrate the potential of using kinetic ^{1}H-^{13}C HSQC NMR spectroscopy for analysing complex chemical systems. We want to point out that NMR spectroscopy by itself has several strongholds as an analytical tool. There is no need to 'freeze' the dynamic system *via* a covalent post modification, no internal standards are required to correct for different responses (which may occur with HPLC, GC, or MS analysis),‡‡ and the protocol does not need to be optimised for each different library. Using ^{1}H-^{13}C HSQC NMR spectroscopy the size of the chemical library can be significantly increased. Here we have studied a system composed of four hydrazones, but taking into account the presence of two isomers for hydrazones **1A**, **1B**, and **1D**, the actual number of measured species was seven. Considering the large spatial separation of these signals in the 2D 'fingerprint' area (Fig. 1d) this number could even be further increased. However, as a general point, it is clear that the spatial separation of signals is a critical issue for the general application of this technique. To our opinion, adding a 'kinetic' component to 2D NMR spectroscopy pushes its potential for monitoring complex molecular networks to a new level. Not only does it resolve the problem of signal identification, but in a single shot it also gives access to the kinetic and thermodynamic parameters. Finally, it also allows a direct monitoring of the adaptive behavior of a chemical system.

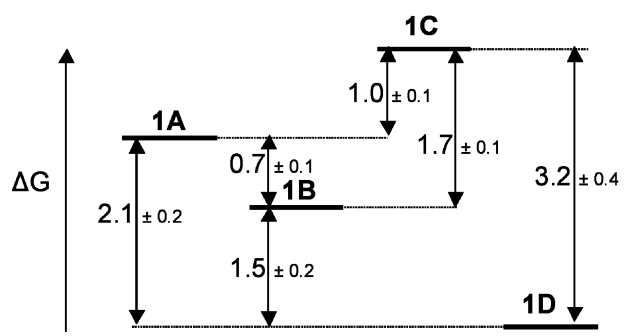

Fig. 3 Thermodynamic stabilities of hydrazones **1A–1D** obtained by extrapolation of the kinetic profile of the third section (Fig. 1d).‖

Support by MIUR (PRIN 2006), the University of Padova (project CPDA054893) and the *Département de l'Instruction Publique* (State of Geneva) is gratefully acknowledged. Most 2D experiments were acquired using the 600 MHz *d'intérêt Romand* located at the Lausanne Polytechnical school (EPFL).

Notes and references

§ Since the two isomers of hydrazones **1A**, **1B**, and **1D** have the same kinetic behavior and have a constant ratio, they are treated as a single species regarding the kinetic and thermodynamic analysis.
¶ New compounds **1C** and **1D** were characterized by ^{1}H, ^{13}C and ESI-MS. See ESI.†
‖ Since intermediate structures are never observed, the thermodynamic equilibrium constant, *e.g.* $K_{\mathbf{1A\rightarrow 1B}}$, is defined as the ratio of the two rate constants for the given equilibrium, *i.e.* $k_{\mathbf{1A\rightarrow 1B}} : k_{\mathbf{1B\rightarrow 1A}}$.
** The differences in heteronuclear carbon–proton coupling constants $^{1}J_{CH}$ turned out to be useful to distinguish the imine C–H from the pyridinium protons.
†† In previous work[9] we had not identified the minor isomer of **1D** (accounting for 20%) due to a lower resolution of the NMR spectrum. However, considering that this was a comparative study with a reference hydrazone this has no effect on the obtained conclusions.
‡‡ Relative intensities between different signals may be affected by different $^{1}J_{HC}$ coupling constants or relaxation rates. In order to verify the effect of these parameters, all signals in Fig. 1 were corrected (see ESI†) and the final thermodynamic composition was determined *via* extrapolation of section 3. A new ratio for [**1A**] : [**1B**] : [**1C**] : [**1D**] of 18 : 24 : 16 : 42 was determined illustrating a maximum difference of only 3% for **1C**.

1. G. M. Whitesides and R. F. Ismagilov, *Science*, 1999, **284**, 89–92.
2. R. F. Ludlow and S. Otto, *Chem. Soc. Rev.*, 2008, **37**, 101–108.
3. J.-M. Lehn, *Chem. Soc. Rev.*, 2007, **36**, 151–160; P. T. Corbett, J. Leclaire, L. Vial, K. R. West, J.-L. Wietor, J. K. M. Sanders and S. Otto, *Chem. Rev.*, 2006, **106**, 3652–3711.
4. V. Patzke and G. von Kiedrowski, *Arkivoc*, 2007, **part v**, 293–310; N. Paul and G. F. Joyce, *Curr. Opin. Chem. Biol.*, 2004, **8**, 634–639.
5. I. R. Epstein, J. A. Pojman and O. Steinbock, *Chaos*, 2006, **16**, 037101.
6. C. J. Kastrup, F. Shen and R. F. Ismagilov, *Angew. Chem., Int. Ed.*, 2007, **46**, 3660–3662; M. K. Runyon, B. L. Johnson-Kerner and R. F. Ismagilov, *Angew. Chem., Int. Ed.*, 2004, **43**, 1531–1536.
7. I. Stahl and G. von Kiedrowski, *J. Am. Chem. Soc.*, 2006, **128**, 14014–14015; R. M. Bennes and D. Philp, *Org. Lett.*, 2006, **8**, 3651–3654.
8. G. Gasparini, M. Martin, L. J. Prins and P. Scrimin, *Chem. Commun.*, 2007, 1340–1342.
9. G. Gasparini, L. J. Prins and P. Scrimin, *Angew. Chem., Int. Ed.*, 2008, **47**, 2475–2479.
10. D. Jeannerat, *J. Mag. Res.*, 2007, **186**, 112–122.
11. B. Levrand, Y. Ruff, J.-M. Lehn and A. Herrmann, *Chem.Commun.*, 2006, 2965–2967; G. Palla, G. Predieri, P. Damiano, C. Vignali and W. Turner, *Tetrahedron*, 1986, **42**, 3649–3654.

